

## INFRAORBITAL NERVE TRANSECTION AND WHISKER FOLLICLE REMOVAL IN ADULT RATS AFFECT MICROGLIA AND ASTROCYTES IN THE TRIGEMINAL BRAINSTEM. A STUDY WITH LIPOCORTIN1- AND S100 $\beta$ -IMMUNOHISTOCHEMISTRY

P. MELZER, M.-Z. ZHANG and J. A. McKANNA\*

Department of Cell Biology, Vanderbilt University School of Medicine, Nashville, TN 37232, U.S.A.

**Abstract**—Transections of the infraorbital nerve in adult rats resulted in progressive alterations of microglia identified by Lipocortin1 immunoreactivity at the sites where the primary afferents terminate, i.e. in the trigeminal brainstem sensory nuclei. Microglia proliferated three- to four-fold. Their cell bodies enlarged and their processes thickened. Microglial responses were similar to the removal of whisker follicles. However, they were restricted to discrete nuclear subregions that matched with the known whisker somatotopy. Astrocytes identified by S100 $\beta$  immunoreactivity showed minor increases in size and in population density. No microglial or astrocytic reactions were found in the second and third synaptic relays of the somatosensory pathway.

Because both types of lesion reportedly lead to the reorganization of primary afferents, our results establish the two experimental designs as valuable tools to elucidate the role of microglia and Lipocortin1 in adult brain plasticity. © 1997 IBRO. Published by Elsevier Science Ltd.

*Key words:* rodent, peripheral nerve, vibrissa, somatosensory system, glial reaction, annexin1.

The whisker-to-barrel pathway is the part of the rodent somatosensory system that connects the receptors in the whisker follicles on the snout to a subdivision of the contralateral primary somatosensory cortex where the whiskers are somatotopically represented by cytoarchitectonic units termed barrels.<sup>41</sup> The pathway projects through the infraorbital branch of the trigeminal nerve to the ipsilateral trigeminal sensory brainstem nuclei. These nuclei are connected with the contralateral thalamic ventro-posterior medial nucleus, from which projections rise to terminate in barrel cortex.

After the transection of the infraorbital nerve in adults myelinated nerve fibres in the proximal nerve stump survive<sup>39</sup> and reinnervate their peripheral targets.<sup>32</sup> Eventually, only 14% of the Gasserian ganglion cells die,<sup>2</sup> and the primary afferents to the brainstem regain responses to whisker stimulation.<sup>33</sup> However, the originally precise somatotopy of their circumscribed endings disintegrates into a diffuse, disorderly pattern.<sup>6</sup> Furthermore, neuronal receptive fields are significantly larger than normal and a few are anomalously split.<sup>21</sup>

This reorganization of afferents may involve microglia. Microglia in the caudal trigeminal sensory brainstem have been shown to react to infra-

orbital nerve transection.<sup>15</sup> Elaborating on this finding, we investigated whether lesions in the trigeminal sensory periphery activate microglia in all nuclei of termination and, perhaps, in the post-lemniscal stations of the whisker-to-barrel pathway. Microglia were stained with immunohistochemistry for Lipocortin1 (LC1), a member of the annexin family of Ca<sup>2+</sup>- and phospholipid-binding proteins that was discovered as a putative mediator of the anti-inflammatory actions of glucocorticoids.<sup>17</sup> In the rat brain, LC1 is predominantly expressed in microglia.<sup>25,28</sup> The microglial reaction was compared with that of astrocytes identified by immunohistochemistry for the Ca<sup>2+</sup>-binding protein S100 $\beta$ .<sup>25</sup>

Two types of lesion were employed: i) transection of the infraorbital nerve and ii) surgical removal of selected whisker follicles. In contrast to the traditionally used transections of motor nerves<sup>22</sup> or mixed motor and sensory nerves,<sup>36</sup> these types of lesion only impair the peripheral processes of Gasserian ganglion cells and do not directly affect neurons in the CNS. Moreover, lesions of peripheral nerves do not disrupt the blood-brain barrier and reduce the potential invasion of brain tissue by blood-borne macrophages that may interfere with the glial response. Preliminary findings of the present study have appeared in abstract form.<sup>31</sup>

\*To whom correspondence should be addressed.

*Abbreviations:* CTR, control; LC1, Lipocortin1.

## EXPERIMENTAL PROCEDURES

### The lesions

All experiments were carried out in accordance with the NIH Guide for the Care and Use of Laboratory Animals. Adult female and male Long-Evans rats were used in this study. On the snout of the rat five rows of tall caudal whiskers, named A (dorsal) to E (ventral), are prominent. The rows are straddled caudally by four solitary whiskers. The whiskers in each row are numbered beginning at the caudal end with 1. In three rats the right side of the snout remained unoperated as control (*CTR*). On the left side, two animals had the follicles of whiskers C1, C2 and C3 (C1–3) surgically removed under ketamine anaesthesia (50 mg/kg i.m.) and the third animal had all whisker follicles deafferented by the transection of the infraorbital nerve at the infraorbital foramen. These animals were allowed to survive four days in 12 h/12 h light/dark cycles with food and water *ad libitum*. Because the glial reaction to the lesions remained restricted to the ipsilateral brainstem, both sides were regarded to be independent from each other in the subsequent experiments. Sixteen rats had the follicles of whiskers C1–3 removed on the right side. On the left side, either the follicles of whiskers B1–3 and D1–3 were removed (four rats) or the infraorbital nerve was transected (eight rats). These rats were housed under the conditions described above four, 14, 30 and 60 days. At each time interval, two rats with nerve transections and one rat that had whisker follicles removed were killed.

### Immunohistochemistry

The rats were killed with pentobarbital (80 mg/kg i.p.), injected i.p. with heparin (1000 units/kg) and transcardially perfused with 50 ml saline, containing heparine (1000 units) and 0.01% NaNO<sub>2</sub>, followed by 150 ml GPAS [glutaraldehyde (2.5%); periodate sodium (10 mM); acetic acid (1.0%); phosphate-buffered saline (0.9% NaCl in 40 mM buffer)]. The brains were removed, postfixed and embedded in paraffin. Alternate series of 10- $\mu$ m-thick sections were obtained. Sections through the brainstem were cut transversely or horizontally. Sections through the thalamus were cut coronally. Sections through cortex were cut tangentially to the pial surface or coronally. Sections through the whiskerpads were cut parallel to the surface of the skin. After deparaffinization, the sections were immunostained using 1:8000 dilutions of polyclonal rabbit antisera raised against

human placental LC1<sup>1</sup> or S100 $\beta$ .<sup>38</sup> Then the sections were stained for Nissl substance.

### Data assessment

The stained sections were scrutinized for changes in morphology and in areal population density of immunoreactive glia under a microscope (Ortholux, Leitz, Wetzlar,

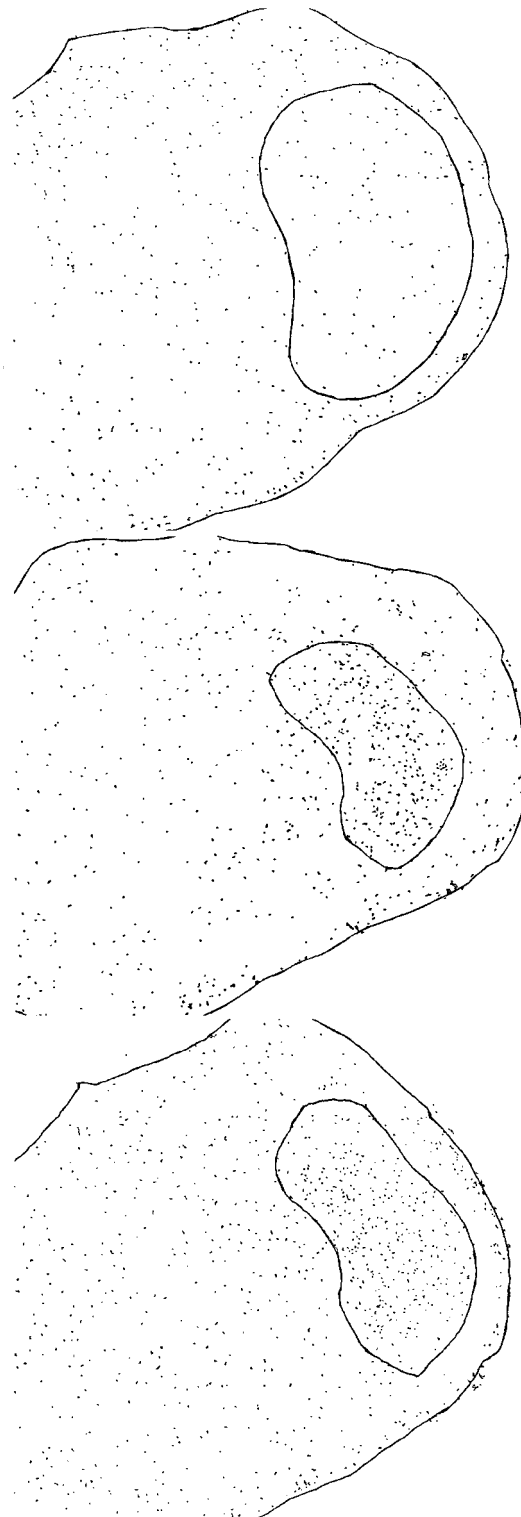


Fig. 1. Microglial reaction in subnucleus interpolaris after the transection of the infraorbital nerve. Middle column: low-power micrographs of transverse sections immunostained for LC1 (Scale bars=400  $\mu$ m). The days of survival after the nerve transection are indicated at the lower centre of each micrograph. *CTR* is from an unoperated side. Left column: Maps of microglial profiles from the sections shown in the micrographs. The outlines in the sections delineate the subnucleus. Right column: high-power micrographs taken within the subnucleus (Scale bars=20  $\mu$ m). Note the increase in the number of LC1-immunoreactive microglia ipsilateral to the lesion beginning four days after nerve transection (4<sup>d</sup>). The microglia were attached to perikarya more frequently and with more and thicker processes (small filled arrows) than in the control. Fourteen days after the lesion LC1-immunoreactive microglia remained numerous (14<sup>d</sup>). A few chromatolytic neurons were detected (large filled arrows). At 30 (30<sup>d</sup>) and 60 days (60<sup>d</sup>) still more LC1-immunoreactive microglia were present than in the controls. However, 60 days after nerve transection not all LC1-immunoreactive cell bodies belonged to microglia. We found a few large perikarya (60<sup>d</sup>; open arrow). These cell bodies may belong to neurons undergoing apoptosis. Orientation: dorsal is up; the animal's left side is on the right.

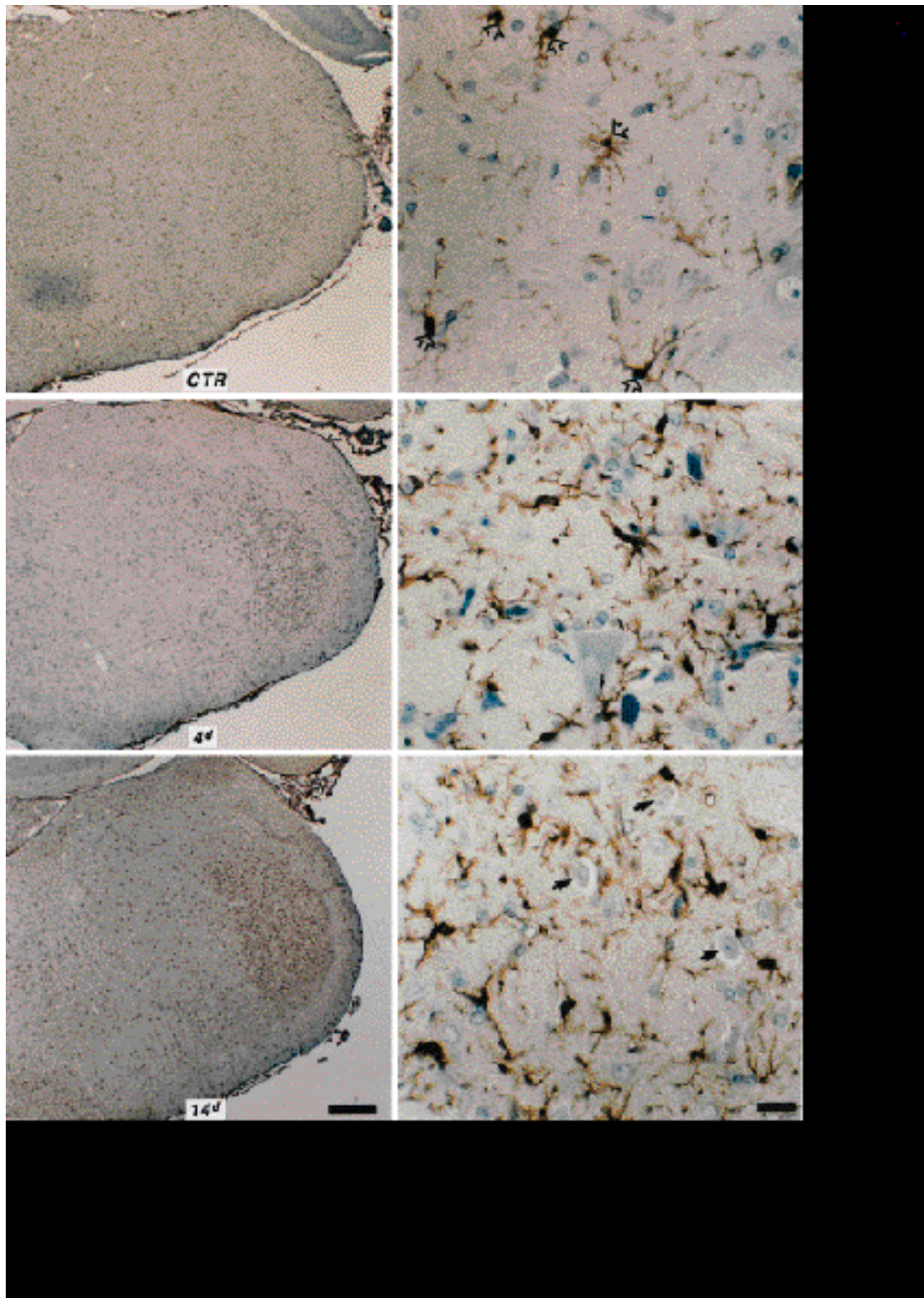


Fig. 1 (continued).

Germany). The glial profiles were mapped on video images digitized with a computerized image analysis system (Bioquant, R&M Biometrics Inc., Nashville, TN, U.S.A.). Only profiles above a pre-determined size and staining intensity were captured. The thresholds were set empirically to exclude partially cut cell bodies and processes. Trigeminal brainstem subnucleus caudalis, subnucleus interpolaris and nucleus principalis as well as the thalamic ventroposterior medial nucleus were outlined, their areal extent in  $\mu\text{m}^2$  was measured, the number of stained cells within each nuclear outline was counted, and the glial population density was calculated. The measurements from several sections/nucleus were highly consistent. However, to minimize the potential influence of cell body enlargement the result of only one section from the rostrocaudal middle of each nucleus was chosen to represent its glial population density. The time-course of the microglial reaction in the three trigeminal brainstem nuclei was illustrated by plotting the nuclear cell population densities of each rat versus the time interval after the lesion.

In order to assess the potential influence of microglial cell body enlargement on the measurement of cell population density, cell body diameters were measured with a calibrated graticule under the microscope in subnucleus caudalis and subnucleus interpolaris of the animals with the greatest microglial population densities four and 60 days after nerve transection. The measurements were carried out in five non-overlapping fields of standard size on one section/nucleus ipsilateral and, in the case with an unoperated side, contralateral to the lesion. The cell bodies were counted, and the percentage of the number of cell bodies larger than  $10 \mu\text{m}$  was calculated.

## RESULTS

In the present study, microglia and astrocytes were identified immunohistochemically with antibodies against LC1 or S100 $\beta$ . Infraorbital nerve transection and whisker follicle removal resulted in alterations of microglial morphology and population density at the sites where the primary trigeminal afferents terminate. The observed alterations of astrocytes, however, remained small. Below, emphasis is given to the microglial reactions in the three structures with strong somatotopic input, i.e. subnucleus caudalis, subnucleus interpolaris and nucleus principalis. No glial reactions could be detected at the second and third synaptic relay stations of the pathway, i.e. the thalamic ventroposterior medial nucleus and the barrel cortex, respectively. No differences in glial reaction were found in animals that were subjected to the same types of lesion on opposite sides.

### *Nerve transection*

**Changes in microglial morphology.** On the unoperated sides, a few microglia were scattered throughout subnucleus interpolaris (Fig. 1, *CTR*), subnucleus caudalis (Fig. 2, *CTR*) and nucleus principalis. They had small, clearly separated cell bodies (none was larger than  $10 \mu\text{m}$  in diameter) with ramified processes. A similar microglial appearance was found in the thalamic ventroposterior medial nucleus and the barrel cortex on the contralateral side.

Four days after the nerve transection, the morphology of microglia was changed throughout the

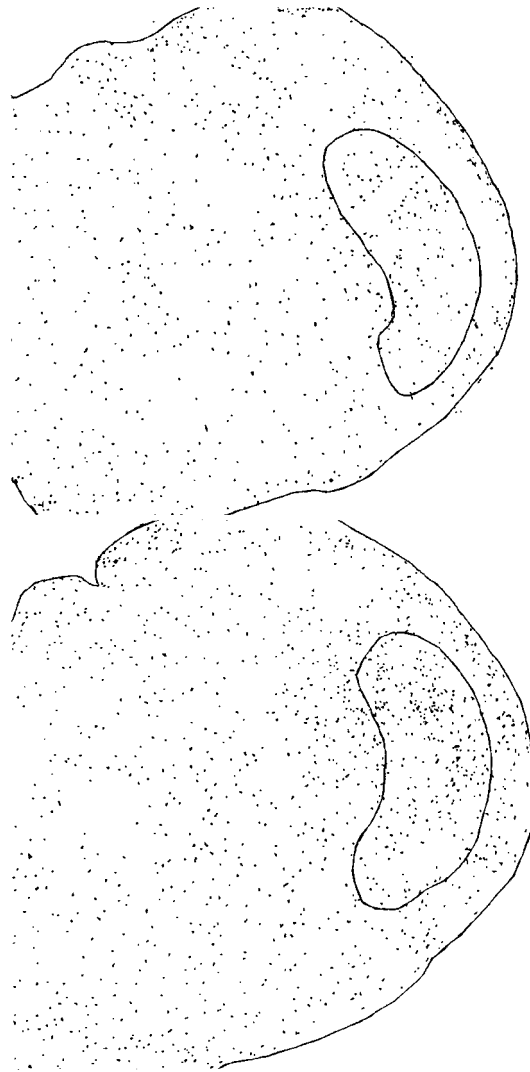


Fig. 1 (*continued*).

rostrocaudal extent of the three brainstem nuclei ipsilateral to the lesion. The processes of the microglia appeared thickened near the cell body and were in contact with perikarya more frequently than in unoperated controls. No microglial alterations were observed in either thalamic ventroposterior medial nucleus or barrel cortex.

Fourteen days after nerve transection, the microglia were in the state observed at four days. Apparently, small-scale degeneration of postsynaptic neuronal elements had begun, since a few chromatolytic neurons<sup>10</sup> were observed (Fig. 1, *14<sup>d</sup>*; arrows).

Thirty days after nerve transection the cell bodies of many microglia were ovoid. Their processes appeared shorter and less arborized than at 14 days (Figs 1, 2, *30<sup>d</sup>*).

Sixty days after nerve transection the appearance of microglia did not differ from that at 30 days. On rare occasions, LC1 immunoreactivity was apparent in isolated neurons interspersed among the microglia



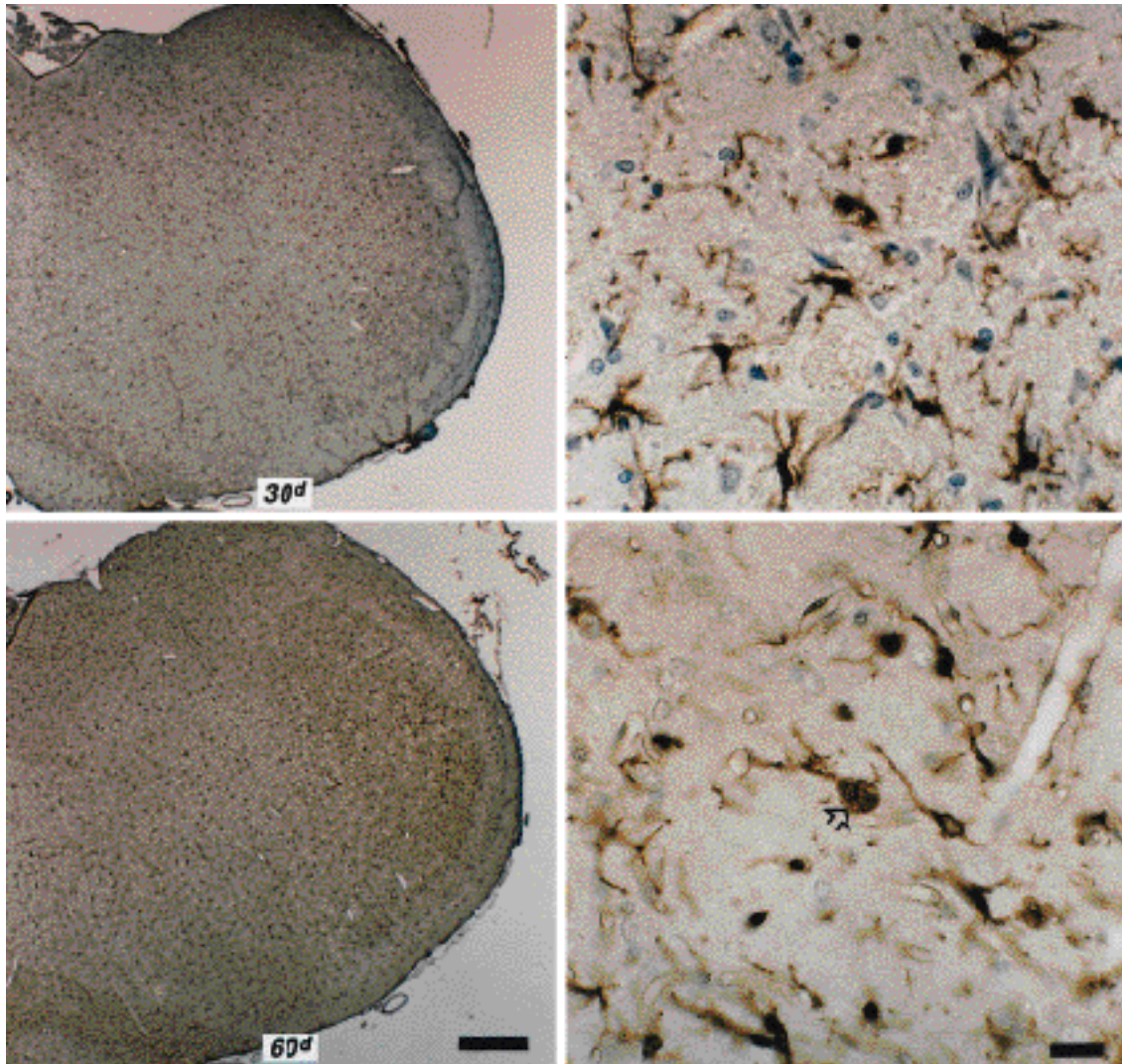


Fig. 1 (continued).

(Fig. 1, 60<sup>d</sup>; unfilled arrow). Possibly, this LC1 is related to neuronal apoptosis.<sup>26</sup>

Although the shapes and numbers of microglia showed clear differences in subnucleus interpolaris (Fig. 1, left column) and nucleus principalis (Fig. 3, right column) at all time intervals after nerve transection, the distribution of microglia remained roughly uniform. In contrast, in subnucleus caudalis microglia appeared distinctly more concentrated in superficial layers I and II than in the deeper layers four days after the lesion (Figs 2, 3, 4<sup>d</sup>) whereas no such difference was observed at the longest time interval after the lesion examined, i.e. 60 days (Figs 2, 3, 60<sup>d</sup>).

*Changes in microglial population density.* In the non-deafferented trigeminal brainstem and thalamus, the microglial population densities were in the range of the 1.0–1.5 cells/100  $\mu\text{m}^2$  found in the normal rat.<sup>25</sup> Four days after nerve transection the average

population density in subnucleus caudalis, subnucleus interpolaris and nucleus principalis ipsilateral to nerve transection ranged from 3–4 cells/100  $\mu\text{m}^2$  (Fig. 4). This increase reflected predominantly cell proliferation, because in the rat with the greatest microglial population density only 9  $\pm$  6% (mean  $\pm$  S.D.) of the microglia in subnucleus caudalis and 10  $\pm$  3% of the microglia in subnucleus interpolaris had cell bodies larger than 10  $\mu\text{m}$ . In the contralateral thalamic ventroposterior nucleus, the microglial population density was at 1.0 cell/100  $\mu\text{m}^2$  in the normal range. At 14 days the population density in the three brainstem nuclei consolidated at  $\sim$ 3.5 cells/100  $\mu\text{m}^2$ . At 30 days it had diminished to  $\sim$ 2 cells/100  $\mu\text{m}^2$ , and this elevated level persisted up to 60 days. At that time interval, 22  $\pm$  8% (mean  $\pm$  S.D.) of the microglia in subnucleus caudalis and 19  $\pm$  10% of the microglia in subnucleus interpolaris of the animal with the greatest cell population density had



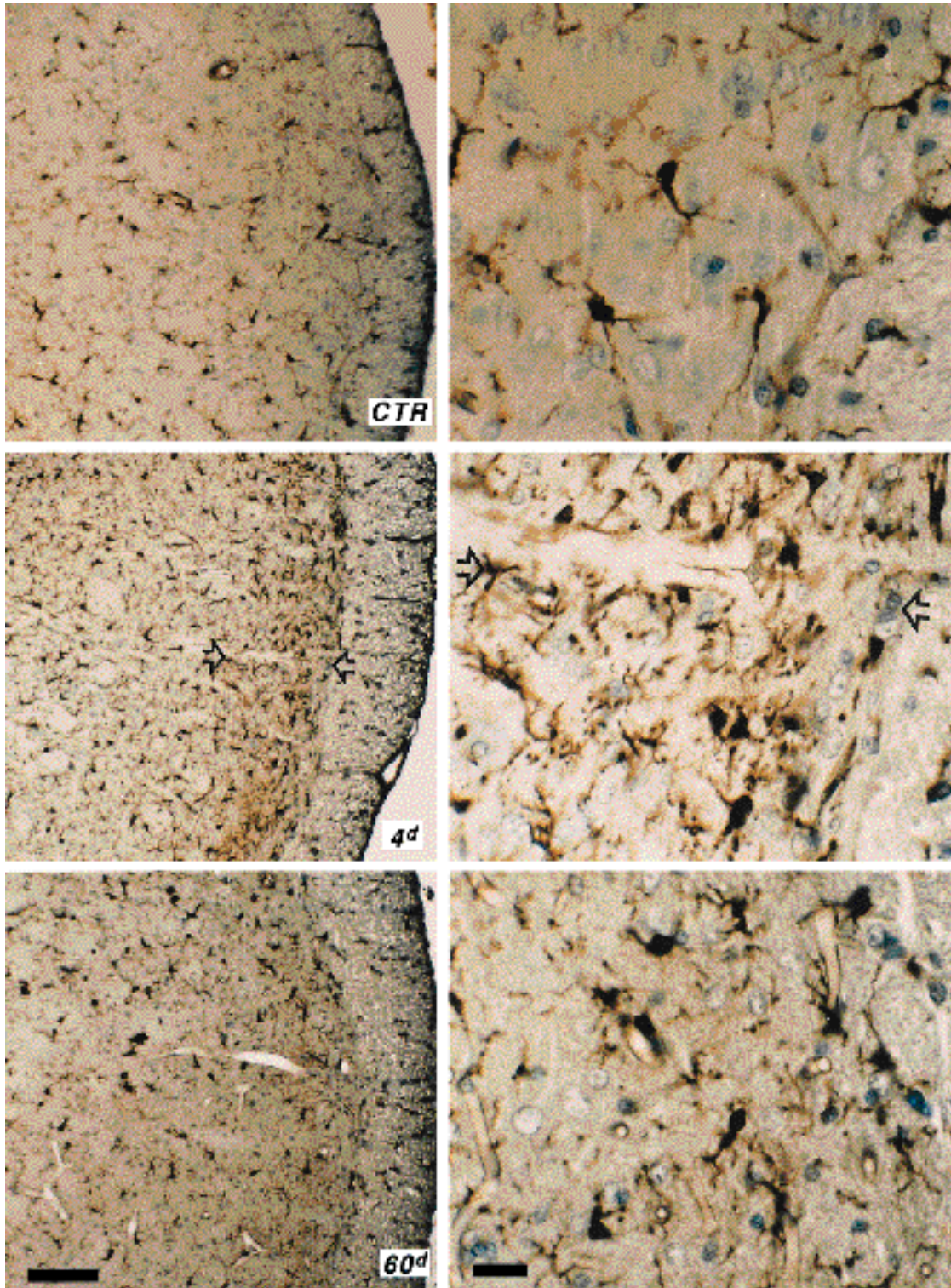


Fig. 2. Microglial reaction in subnucleus caudalis after the transection of the infraorbital nerve. Left column: low-power micrographs of transverse sections immunostained for LC1 (scale bar=100  $\mu$ m). The days of survival after the nerve transection are indicated at the lower right of each micrograph. *CTR* is from an unoperated side. Right column: high-power micrographs taken within the subnucleus (Scale bar=20  $\mu$ m). Four days after nerve transection, the number of LC1-immunoreactive microglia was increased on the ipsilateral side (*4<sup>d</sup>*). A distinct rim of greater cell concentration spanned layers I and II (between the arrows in the right column). The distribution of cells became more homogenous with increasing survival time. Orientation: dorsal is up; the animal's left side is on the right.

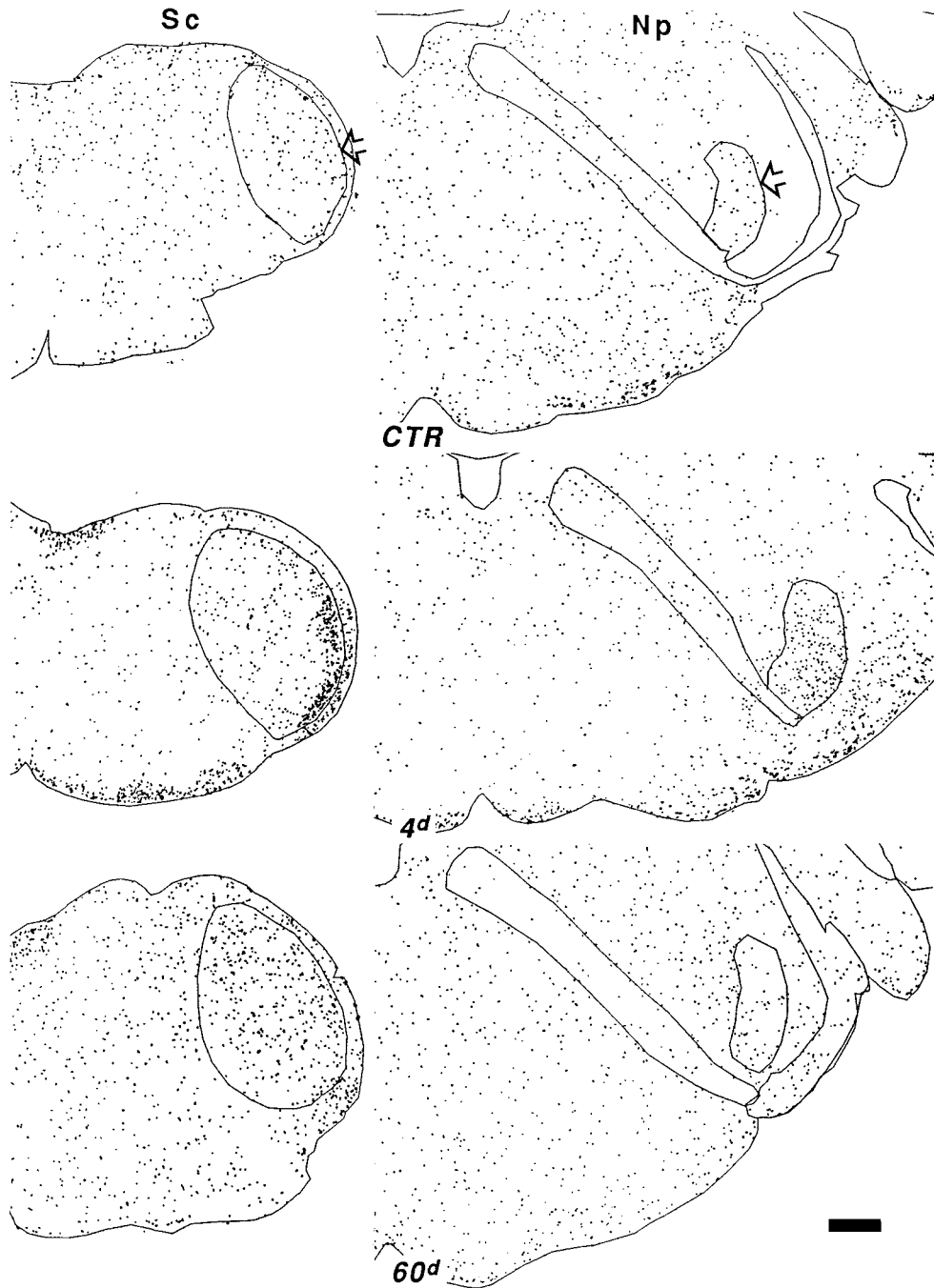


Fig. 3. Maps of microglia in subnucleus caudalis and nucleus principalis after the transection of the infraorbital nerve. LC1-immunoreactive cellular profiles were mapped on transverse sections through subnucleus caudalis (Sc) and nucleus principalis (Np). The days of survival after the nerve transection are indicated at the lower centre of each row of panels. *CTR* is from an unoperated side. The two nuclei are outlined (arrows) and major white matter tracts are delineated in the maps of Np. Four days after nerve transection the number of LC1-immunoreactive microglia was increased in both nuclei on the ipsilateral side (*4<sup>d</sup>*). Note the aggregation of microglia in the superficial layers of subnucleus caudalis at four days (*4<sup>d</sup>*), which was absent 60 days after nerve transection (*60<sup>d</sup>*). Orientation: dorsal is up; the animal's left side is on the right. Scale bar=400  $\mu$ m.

cell bodies larger than 10  $\mu$ m in diameter. Therefore, microglial enlargement does not account for the measured increases in cell population density at 60 days.

#### *Whisker follicle removal*

The histological examination of the whiskerpads confirmed that the selected whisker follicles were

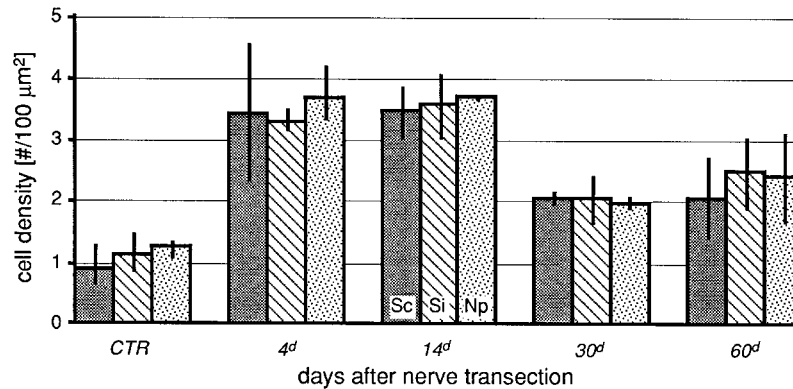


Fig. 4. Effect of infraorbital nerve transection on the areal density of LC1-immunoreactive microglia in subnucleus caudalis (Sc), subnucleus interparialis (Si) and nucleus principalis (Np). The mean cell population density derived from profile mapping is plotted versus the days of survival after the lesion. The bars represent the ranges. *CTR* designates data from unoperated sides. In comparison with *CTR*, the nuclear population densities of immunoreactive microglia were increased by about 3–4-fold at four (*4<sup>d</sup>*) and 14 days (*14<sup>d</sup>*). The densities were diminished to a level twice that of *CTR* 30 (*30<sup>d</sup>*) and 60 days (*60<sup>d</sup>*) after nerve transection.

completely removed by the surgical excisions. Follicle removal resulted in an increase in the population density of microglia immunoreactive for LC1 in circumscribed subregions along the rostrocaudal extent of ipsilateral subnucleus caudalis, subnucleus interparialis and nucleus principalis. The increase was most prominent four days after the lesion and similar in the three nuclei. Therefore, the effects of whisker follicle removal are exemplified by the glial reaction in subnucleus interparialis.

After the removal of the follicles of whiskers B1–3 and D1–3 the population density of LC1-immunoreactive microglia increased in two discrete regions. In the transverse plane, they appeared as separate, narrow bands extending lateromedially. One was located dorsally and the other ventrally in the subnucleus (Fig. 5, *B1–3* and *D1–3*). In contrast, the removal of the follicles of whiskers C1–3 led to only one band of increased microglial population density at the dorsoventral middle of the subnucleus (Fig. 5, *C1–3*). The location of this band was complementary to the locations of the two bands found after the removal of the follicles of whiskers B1–3 and D1–3. No attempt was undertaken to quantify these local changes because of the lack of morphological landmarks to delimit the loci.

#### *Comparison of microglia and astrocytes*

Consistent with the reliable identification of astrocytes by S100 $\beta$ , staining for S100 $\beta$  immunoreactivity demonstrated a population of cells distinctly different from LC1-immunoreactive microglia. At all survival times examined, the cell bodies of S100 $\beta$ -immunoreactive astrocytes were more spherical and contained larger, rounder, more uniformly shaped nuclei than the LC1-immunoreactive microglia (Fig. 6). The average population density of astrocytes on the unoperated side was  $\sim 2.9$  glia/100  $\mu\text{m}^2$ , a value

comparable to that reported by McKanna<sup>25</sup> for normal rats. After the removal of whisker follicles, astrocytes did not change in appearance and in population density. However, after nerve transection we observed minor increases in the size of their cell bodies and in their population density, i.e.  $\sim 3.5$  glia/100  $\mu\text{m}^2$  at four days and  $\sim 3.7$  glia/100  $\mu\text{m}^2$  at 60 days.

#### DISCUSSION

The present study demonstrates that after the alteration of trigeminal sensory inputs to the nuclei of termination of adult rats LC1-immunoreactive cells undergo the distinct morphological changes and the prominent increase in areal population density that are typical of a microglial reaction. In contrast, S100 $\beta$ -immunoreactive cells, i.e. astrocytes, showed minimal changes.

The clear dichotomy in localization between LC1 and S100 $\beta$  permits an unambiguous distinction between mature microglia and astrocytes. Co-expression of these two proteins is observed only in ependyma and blast cells of the adult subventricular zone.<sup>27</sup> Also, recent evidence indicates that another isoform, S100C, binds specifically to LC1.<sup>24</sup>

No microglial reaction was found in the second and third synaptic relay stations of the whisker-to-barrel pathway, i.e. in the somatosensory thalamus and cortex. Topper *et al.*<sup>37</sup> observed microglial reactions in diencephalic, but not in mesencephalic, second order nuclei after cytotoxic lesions in the striatum. These authors attributed the discrepancy to differences in the strength of the nigral projections. Perhaps, in the present study the degenerating neurons in the nuclei of termination were too few to trigger a microglial reaction in the second synaptic relay station.



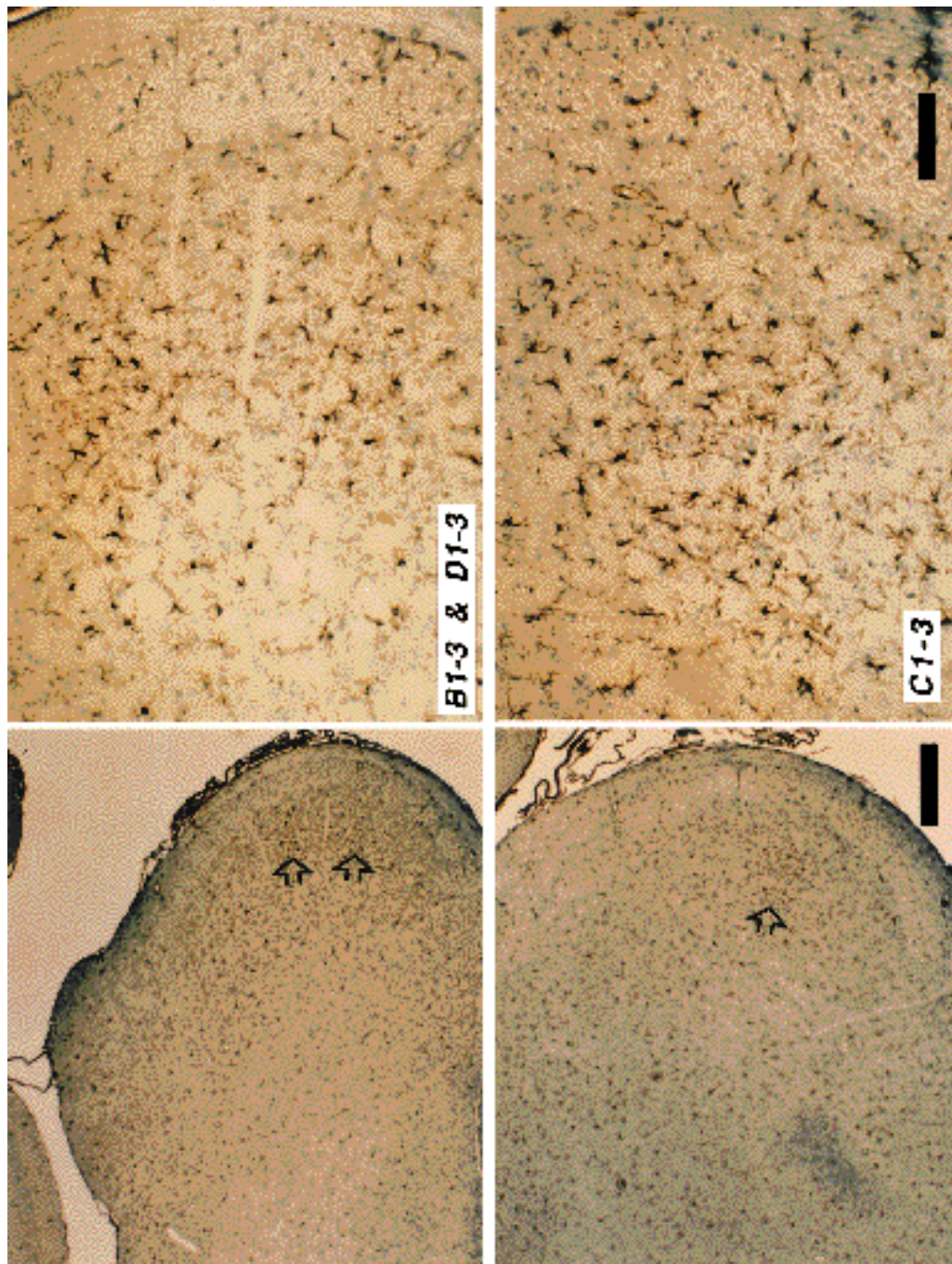


Fig. 5. Microglial reaction in subnucleus interparietalis after whisker follicle removal. Effects of the removal of the follicles of whiskers B1-3 and D1-3 (top row of panels) and C1-3 (bottom row of panels) four days after the lesion. Left column: low-power micrographs of transverse sections immunostained for LC1 (Scale bar=400  $\mu$ m). The removal of whisker follicles in two rows resulted in two distinctly separate aggregations of LC1-immunoreactive microglia in subnucleus interparietalis whereas the removal of whisker follicles in one row led to only one such focus. Right column: high-power micrographs taken within the subnucleus demonstrating the complementarity of the two distributions of immunoreactive cells (scale bar=100  $\mu$ m). Orientation: dorsal is up; the animal's left side is on the right.



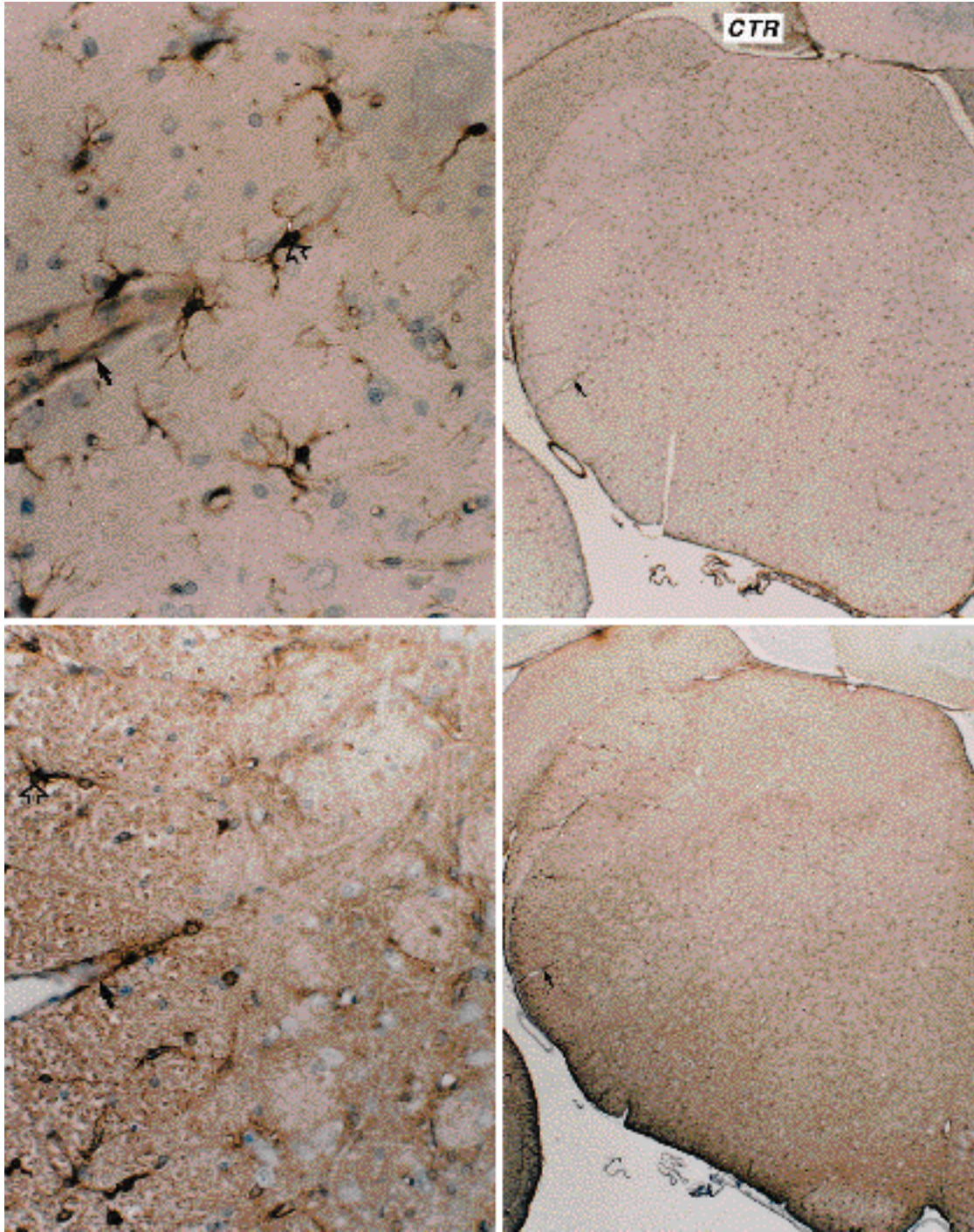


Fig. 6. Comparison of microglia and astrocytes in subnucleus interpolaris. Results from a rat that was killed four days after the removal of left whiskers C1-3. The right side remained unoperated. Inner columns: low-power micrographs of adjacent transverse sections immunostained for microglia (LC1, top row) and for astrocytes (S100 $\beta$ , bottom row) ipsi- (C1-3) and contralateral (CTR) to the lesion (scale bar=400  $\mu$ m). Outer columns: high-power micrographs taken in the subnucleus near the vessels marked with large filled arrows (scale bar=20  $\mu$ m). Microglia had small polymorphic nuclei and were present in the subnucleus on both sides (unfilled arrows). Astrocytes had large round nuclei and were predominantly found laterally to and outside the boundary of the subnucleus (unfilled arrows). In the portions of the subnucleus near the vessels marked with large filled arrows, the population density of microglia on the side with the lesion seemed higher and microglia were less evenly spaced than on the unoperated side. The microglia ipsilateral to the lesion appeared to have thicker processes, were in closer proximity with each other and seemed to contact perikarya more frequently (small filled arrow) than those contralateral to the lesion. In contrast, astrocytes remained unaffected by the lesion. Orientation: dorsal is up; the animal's left side is on the right.



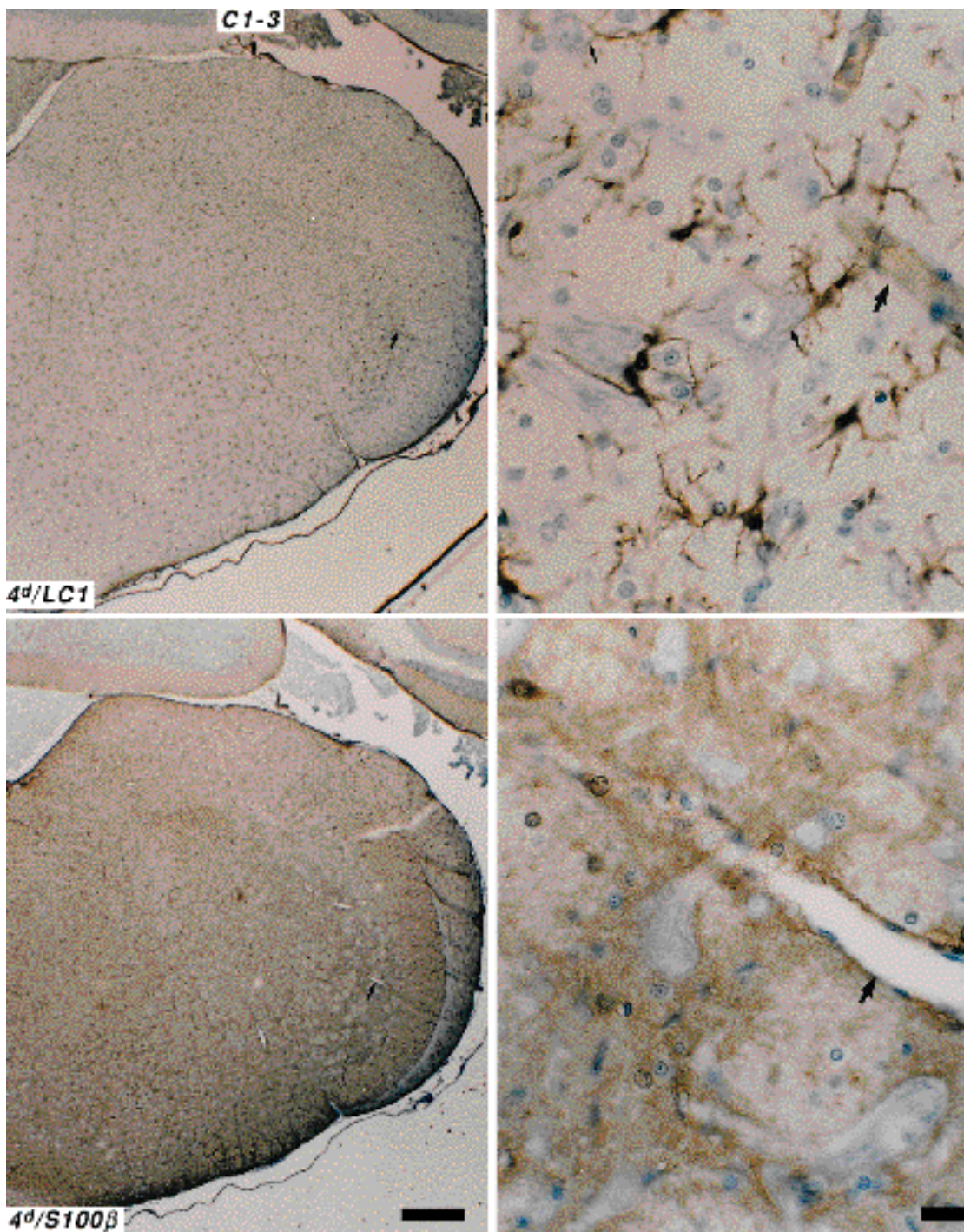


Fig. 6 (continued)

#### Nerve transection

Mapping of LC1-immunoreactive cell profiles indicated that the population density of microglia in the trigeminal brainstem nuclei had about quadrupled four days after the transection of the infra-orbital nerve and diminished to about twice that of unoperated sides at 30 days, a magnitude at which it remained even 60 days after the lesion. A similar evolution of the microglial reaction to infraorbital

nerve transection has been reported by Eriksson *et al.*<sup>15</sup> who measured the surface area occupied by OX42-positive cell profiles on transverse sections through subnucleus caudalis.

Though the use of immunoreactive profiles to measure population density is prone to be confounded by an increase in the size of microglia, in the present study only 10–20% of the microglial cell bodies enlarged to diameters  $>10\ \mu\text{m}$ , and other



studies<sup>19,34,35</sup> have demonstrated that microglia indeed proliferate after peripheral nerve lesions.

The reduction in the number of microglia at 30 and 60 days is consistent with a report of Gehrmann and Banati<sup>19</sup> that some microglia contain fragments of single-stranded DNA after nerve transection and, thus, may be apoptotic. However, the effect of the apoptosis must be minor, because an elevated number of microglia persists even 60 days after the lesion.

The concentration of microglia in layers I and II of subnucleus caudalis four days after nerve transection is an unprecedented finding. It implicates a particular role for thin nociceptive C-fibres that terminate mainly in these layers whereas thick mechanoreceptive afferents terminate in the deeper layers.<sup>18</sup> The differential microglial reaction suggests that nociceptive afferents respond to nerve transection more rapidly and more vigorously than mechanoreceptive afferents.

The thickening of the distal processes of microglia four days after nerve transection is typical of the known microglial transformation from the resting into the activated state.<sup>7,12</sup> Microglial cell bodies were enlarged, possibly because microglia phagocytose degenerating primary afferents.<sup>3,5</sup> Some of the LC1-immunoreactive cells resembled macrophages, though most likely they were phagocytic microglia, because macrophages of monocytic origin are extremely rare in the CNS;<sup>11,20</sup> both observations *in situ* and tissue culture experiments suggest that the microglia identified by LC1 immunoreactivity stem from progenitor cells of neuroepithelial origin.<sup>16,27</sup>

#### *Whisker follicle removal*

The removal of three whisker follicles was sufficient to evoke a microglial reaction in the nuclei of termination. The reactive regions were small and restricted. Their limited extent was similar to that of transganglionic degeneration demonstrated with the Fink-Heimer method eight to 14 days after deafferentation of whisker follicles.<sup>5</sup> In analogy to barrels in layer IV of primary somatosensory cortex,<sup>41</sup> morphological units represent the whiskers on the snout topologically in subnucleus caudalis, subnucleus interpolaris and nucleus principalis.<sup>23</sup> In transverse sections, the units representing the five rows of large caudal whiskers appear as rows of segments rich in the metabolic enzymes cytochrome oxidase<sup>8</sup> and succinic dehydrogenase.<sup>9,14</sup> In the three nuclei, whisker row A is represented ventrally and row E dorsally. The locations of the microglial reactions found in the present study were in good agreement with this map. The extent of the microglial reactions matches that of the terminal fields of primary afferents,<sup>4</sup> and this high degree of spatial confinement demonstrates clearly that the signal for the

microglial reaction remains localized in the direct vicinity of the endings of the deprived afferents.

#### *Persistence of the microglial reaction*

Even at the longest time interval after nerve transection examined, i.e. 60 days, microglia in the trigeminal brainstem nuclei had ovoid cell bodies and short, thick processes distinctly different from unoperated controls. The persistence of this activated state may be associated with the reorganization of primary afferents as a consequence of the protracted reinnervation of the sensory periphery. Renshan and Munger<sup>32</sup> observed that 14 days after infraorbital nerve transection the nerve fibres innervating whisker follicles had degenerated completely; the first regenerated axons, however, were arriving. The reinnervation of follicular receptors was most prominent at 60 days and continued at a smaller rate until 150 days after nerve transection, i.e. the longest time interval studied. Concomitantly, the terminal fields of whisker follicle-specific primary afferents enlarge.<sup>6</sup> This enlargement could be the sole result of erroneous follicular reinnervation.<sup>33</sup> However, the disintegration of nerve fibres in the nuclei of termination and their phagocytosis by glia observed with electron microscopy<sup>3,5</sup> suggest that primary afferents break down. There are indications that they may regenerate novel terminations. Deoxyglucose studies showed that whisker follicle removal<sup>29</sup> or transection of a row nerve<sup>30</sup> in adult mice result in the reshaping of the functional somatotopic representation of whiskers in the trigeminal brainstem. Such reshaping may be the result of an enlargement of the terminal fields of primary afferents similar to the sprouting observed with anatomical tract tracing and electrophysiological recordings in the dorsal horn of the spinal cord after the transection of the sciatic nerve.<sup>13,40</sup> Though the development of novel terminal fields after infraorbital nerve transection in adults remains to be demonstrated, the findings above and the presence of LC1-immunoreactive microglia months beyond the degenerative phase advocate the possibility that such microglia are not only involved in the removal of the debris of neuronal degeneration, but may also play a role in the facilitation of the reorganization of primary afferents.

#### CONCLUSION

Our findings implicate a major participation of LC1-immunoreactive microglia in the reorganization of the mature whisker-to-barrel pathway after a lesion in the sensory periphery. Our study presents two promising models, i.e. reorganization of afferents after nerve transection and reorganization of afferents after whisker follicle removal, that permit the investigation of the role of LC1 and microglia in adult plasticity.

## REFERENCES

1. Ahn N. G., Teller D. C., Bienkowski M. J., McMullen B. A., Lipkin E. W. and De Haen C. (1988) Sedimentation equilibrium analysis of five lipocortin-related phospholipase A2 inhibitors from human placenta. Evidence against a mechanistically relevant association between enzyme and inhibitor. *J. Biol. Chem.* **263**, 18657–18663.
2. Aldskogius H. and Arvidsson J. (1978) Nerve cell degeneration and death in the trigeminal ganglion of the adult rat following peripheral nerve transection. *J. Neurocytol.* **7**, 229–250.
3. Arvidsson J. (1979) An ultrastructural study of transganglionic degeneration in the main sensory trigeminal nucleus of the rat. *J. Neurocytol.* **8**, 31–45.
4. Arvidsson J. (1982) Somatotopic organization of vibrissae afferents in the trigeminal sensory nuclei of the rat studied by transganglionic transport of HRP. *J. Comp. Neurol.* **211**, 84–92.
5. Arvidsson J. (1986) Transganglionic degeneration in vibrissae innervating primary sensory neurons of the rat: a light and electron microscopic study. *J. Comp. Neurol.* **249**, 392–403.
6. Arvidsson J. and Johansson K. (1988) Changes in the central projection pattern of vibrissae innervating primary sensory neurons after peripheral nerve injury in the rat. *Neurosci. Lett.* **84**, 120–124.
7. Banati R. B. and Graeber M. B. (1994) Surveillance, intervention and cytotoxicity: is there a protective role of microglia. *Dev. Neurosci.* **16**, 114–127.
8. Bates C. A. and Killackey H. P. (1985) The organization of the neonatal rat's brainstem trigeminal complex and its role in the formation of central trigeminal patterns. *J. Comp. Neurol.* **240**, 265–287.
9. Belford G. R. and Killackey H. P. (1979) Vibrissae representation in subcortical trigeminal centers of the neonatal rat. *J. Comp. Neurol.* **183**, 305–322.
10. Bodian D. and Mellors R. C. (1945) The regenerative cycle of motoneurons with special reference to phosphatase activity. *J. Exp. Med.* **81**, 469–488.
11. de Groot C. J., Huppes W., Sminia T., Kraal G. and Dijkstra C. D. (1992) Determination of the origin and nature of brain macrophages and microglial cells in mouse central nervous system, using non-radioactive *in situ* hybridization and immunoperoxidase techniques. *Glia* **6**, 301–309.
12. del Río-Hortega P. (1932) Microglia. In *Cytology and Cellular Pathology of the Nervous System* (ed. Penfield W.), Vol. 2, pp. 481–534. P. B. Hoeber Inc., New York.
13. Devor M. and Wall P. D. (1981) Plasticity in the spinal cord sensory map following peripheral nerve injury in rats. *J. Neurosci.* **1**, 679–684.
14. Durham D. and Woolsey T. A. (1984) Effects of neonatal whisker lesions on mouse central trigeminal pathway. *J. Comp. Neurol.* **223**, 424–447.
15. Eriksson N. P., Persson J. K. E., Svensson M., Arvidsson J., Molander C. and Aldskogius H. (1993) A quantitative analysis of the microglial cell reaction in central primary sensory projection territories following peripheral nerve injury in the adult rat. *Expl Brain Res.* **96**, 19–27.
16. Fedoroff S. and McKanna J. A. (1994) Lipocortin-1 is expressed in microglia and their progenitor cells in culture. *Molec. Biol. Cell.* **5**, 228a.
17. Flower R. J. and Rothwell N. J. (1994) Lipocortin 1: cellular mechanisms and clinical relevance. *Trends Pharmacol. Sci.* **15**, 71–76.
18. Fundin B. T., Rice F. L., Pfaller K. and Arvidsson J. (1994) The innervation of the mystacial pad in the adult rat studied by anterograde transport of HRP conjugates. *Expl Brain Res.* **99**, 233–246.
19. Gehrmann J. and Banati R. B. (1995) Microglial turnover in the injured CNS: Activated microglia undergo delayed DNA fragmentation following peripheral nerve injury. *J. Neuropath. Exp. Neurol.* **54**, 680–688.
20. Hickey W. F., Vass K. and Lassmann H. (1992) Bone marrow-derived elements in the central nervous system: An immunohistochemical and ultrastructural survey of rat chimeras. *J. Neuropath. Exp. Neurol.* **51**, 246–256.
21. Klein B. G. (1991) Chronic functional consequences of adult infraorbital nerve transection for rat trigeminal subnucleus interpolaris. *Somatosensory Mot. Res.* **8**, 175–191.
22. Kreutzberg G. W. (1966) Autoradiographische Untersuchungen über die Beteiligung von Gliazellen an der axonalen Reaktion im Facialiskern der Ratte. *Acta neuropath., Berlin* **7**, 149–161.
23. Ma P. and Woolsey T. A. (1984) Cytoarchitectonic correlates of the vibrissae in the medullary trigeminal complex of the mouse. *Brain Res.* **306**, 374–379.
24. Mailliard W. S., Haigler H. T. and Schlaepfer D. D. (1995) Calcium-dependent binding of S100C to the N-terminal domain of annexin I. *J. Biol. Chem.* **271**, 719–725.
25. McKanna J. A. (1993) Lipocortin1 immunoreactivity identifies microglia in adult rat brain. *J. Neurosci. Res.* **36**, 491–500.
26. McKanna J. A. (1995) Lipocortin 1 in apoptosis: mammary regression. *Anat. Rec.* **242**, 1–10.
27. McKanna J. A. and Fedoroff S. (1997) Development of microglia *in situ* and in culture. In *Topical Issues of Microglia* (eds Ling E. A. and Tan A. A.), pp. 21–42. Singapore Neurosci. Ass.
28. McKanna J. A. and Zhang M.-Z. (1997) Immunohistochemical localization of lipocortin 1 in rat brain. *J. Histochem. Cytochem.* **45**, 527–538.
29. Melzer P. and Smith C. B. (1995) Plasticity of the metabolic whisker map in the mouse somatosensory system after follicle removal in neonates and in adults. *J. Cerebr. Blood Flow Metab.* **15 Suppl. 1**, S685.
30. Melzer P., Yamakado M., Van der Loos H., Welker E. and Dörfel J. (1988) Plasticity in the barrel cortex of adult mouse: effects of peripheral deprivation on the functional map; a deoxyglucose study. *Soc. Neurosci. Abstr.* **14**, 844.
31. Melzer P., Zhang M.-Z. and McKanna J. A. (1995) Infraorbital nerve transection and whisker follicle removal result in an increase in reactive microglia in adult rat brainstem trigeminal nuclei. *Soc. Neurosci. Abstr.* **21**, 108.
32. Renehan W. E. and Munger B. L. (1986) Degeneration and regeneration of peripheral nerve in the rat trigeminal system. II. Response to nerve lesions. *J. Comp. Neurol.* **249**, 429–459.
33. Renehan W. E., Chiaia N. L., Klein B. G., Jacquin M. F. and Rhoades R. W. (1989) Physiological and anatomical consequences of infraorbital nerve transection in the trigeminal ganglion and trigeminal spinal tract of the adult rat. *J. Neurosci.* **9**, 548–557.
34. Streit W. J. and Kreutzberg G. W. (1988) Response of endogenous glial cells to motor neuron degeneration induced by toxic ricin. *J. Comp. Neurol.* **268**, 248–263.

35. Svensson M., Mattson P. and Aldskogius H. (1994) A bromodeoxyuridine labelling study of proliferating cells in the brainstem following hypoglossal nerve transection. *J. Anat.* **185**, 537–542.
36. Svensson M., Eriksson P., Persson J. K. E., Molander C., Arvidsson J. and Aldskogius H. (1993) The response of central glia to peripheral nerve injury. *Brain Res. Bull.* **30**, 499–506.
37. Topper R., Gehrmann J., Schwarz M., Block F., Noth J. and Kreutzberg G. W. (1993) Remote microglial activation in the quinolinic acid model of Huntington's disease. *Expl Neurol.* **123**, 271–283.
38. Van Eldik L. J. and Zimmer D. B. (1988) Mechanisms of action of the S100 family of calcium modulated proteins. In *Calcium and Calcium-binding Proteins* (eds Gerday C., Gilles R. and Bolis L.), pp. 114–127. Springer, Berlin.
39. Waite P. M. E. (1984) Rearrangement of neuronal responses in the trigeminal system of the rat following peripheral nerve section. *J. Physiol., Lond.* **352**, 425–445.
40. Woolf C. J., Shortland P. and Coggeshall R. E. (1992) Peripheral nerve injury triggers central sprouting of myelinated afferents. *Nature* **355**, 75–78.
41. Woolsey T. A. and Van der Loos H. (1970) The structural organization of layer IV in the somatosensory region (SMI) of mouse cerebral cortex. The description of a cortical field composed of discrete cytoarchitectonic units. *Brain Res.* **17**, 205–242.

(Accepted 11 December 1996)